Technology in Cancer Research & Treatment
Volume 17: 1-10
© The Author(s) 2018
Article reuse guidelines:
sagepub.com/journals-permissions
DOI: 10.1177/1533033818803632
journals.sagepub.com/home/tct
SAGE

Image-Based Profiling of Patient-Derived Pancreatic Tumor–Stromal Cell Interactions Within a Micropatterned Tumor Model

Shilpaa Mukundan, MS[1], Kriti Sharma[1], Kim Honselmann, MD[2], Amy Singleton, BS[3], Andrew Liss, PhD[2], and Biju Parekkadan, PhD[1,3,4]

Abstract

Pancreatic cancer is one of the most aggressive cancers with a 5-year patient survival rate of 8.2% and limited availability of therapeutic agents to target metastatic disease. Pancreatic cancer is characterized by a dense stromal cell population with unknown contribution to the progression or suppression of tumor growth. In this study, we describe a microengineered tumor stromal assay of patient-derived pancreatic cancer cells to study the heterotypic interactions of patient pancreatic cancer cells with different types of stromal fibroblasts under basal and drug-treated conditions. The population dynamics of tumor cells in terms of migration and viability were visualized as a functional end point. Coculture with cancer-associated fibroblasts increased the migration of cancer cells when compared to dermal fibroblasts. Finally, we imaged the response of a bromodomain and extraterminal inhibitor on the viability of pancreatic cancer clusters surrounding by stroma in microengineered tumor stromal assay. We visualized a codynamic reduction in both cancer and stromal cells with bromodomain and extraterminal treatment compared to the dimethyl sulfoxide-treated group. This study demonstrates the ability to engineer tumor–stromal assays with patient-derived cells, study the role of diverse types of stromal cells on cancer progression, and precisely visualize a coculture during the screening of therapeutic compounds.

Keywords

pancreatic cancer, BET, stroma, tumor microenvironment, microengineered tumor stromal assay (μTSA)

Abbreviations

BET, bromodomain and extraterminal; CAF, cancer-associated fibroblast; DMEM, Dulbecco's modified Eagle medium; DMSO, dimethyl sulfoxide; EGF, epithelial growth factor; NHDF, normal human dermal fibroblast; PBS, phosphate-buffered saline; PDMS, polydimethylsiloxane; μTSA, microengineered tumor stromal assay

Received: March 12, 2018; Revised: July 5, 2018; Accepted: August 7, 2018.

Introduction

Pancreatic cancer remains as one of the most aggressive types of cancers with a very poor patient outcome.[1] Currently, gemcitabine and 5-fluorouracil are the most commonly used chemotherapeutic compounds being used to treat patients, but there is clearly an unmet need to discover new therapies for treating pancreatic cancer. Understanding the key components and drivers of a pancreatic cancer microenvironment can reveal new mechanistic targets to improve cancer therapy. Cancer cells do not live in a vacuum; they are surrounded by several cellular and noncellular components that are emerging as major instigators of tumor growth or tumor suppression and potential targets for therapy.[2,3] Breast, prostate, gastrointestinal, and

[1] Department of Biomedical Engineering, Rutgers, The State University of New Jersey, Piscataway, NJ, USA
[2] Department of Surgery, Andrew L. Warshaw Institute for Pancreatic Cancer Research, Massachusetts General Hospital, Harvard Medical School, Boston, MA, USA
[3] Center for Surgery, Bioengineering, and Innovation, Department of Surgery, Massachusetts General Hospital, Harvard Medical School and the Shriners Hospitals for Children, Boston, MA, USA
[4] Cancer Institute of New Jersey, New Brunswick, NJ, USA

Corresponding Author:
Biju Parekkadan, PhD, Department of Biomedical Engineering, Rutgers, The State University of New Jersey, 599 Taylor Road, Piscataway, NJ 08854, USA.
Email: biju.parekkadan@rutgers.edu

Creative Commons Non Commercial CC BY-NC: This article is distributed under the terms of the Creative Commons Attribution-NonCommercial 4.0 License (http://www.creativecommons.org/licenses/by-nc/4.0/) which permits non-commercial use, reproduction and distribution of the work without further permission provided the original work is attributed as specified on the SAGE and Open Access pages (https://us.sagepub.com/en-us/nam/open-access-at-sage).

pancreatic cancer have abundant amounts of stromal cells when compared to other tumors.[4,5] The stromal compartment undergoes significant changes at all levels from cell phenotype,[6,7] epigenetics,[8] to gene expression profile,[5,6] which are partly accounted for by activation and transdifferentiation of local cells, and partly by recruitment of new cell types into the tumors.[9] Therefore, ideal models for studying cancer therapeutics should be able to follow and interrogate the natural evolution of morphological and compositional characteristics of tumor tissue.

In vivo mouse models are one of the most promising and commonly used models to study drug efficacy within a complex stromalized tumor microenvironment.[6] Despite these properties of animal models, they are time-consuming to develop, low-throughput, and expensive. In addition, genetics, immunological, and cellular disparities exist between humans and mice.[10,11] *In vitro* high-throughput screening of cancer cell lines with an end point such as cytotoxicity is typically used to identify compounds of interest more rapidly. However, these simple cancer models do not account for the heterotypic interaction between cancer cells[7] and paracrine signaling between tumor cells and cells of the microenvironment that can influence drug efficacy. Three-dimensional tumor spheroid models have proven to be promising models to study drug response and tumor progression in a complex cellular environment.[12-14] To study tumor–stromal interactions, spheroid models have been developed by mixing tumor and stromal cells can mimic cell types and the diffusion limits of a tumor mass.[15,16] However, these models do not control the spatial tumor–stromal interactions that exist in the *in vivo* solid tumors. To address this issue, recent studies have focused on the development of microfluidic and hydrogel-based approaches to study cancer–stromal interactions. In a recent study by Hong *et al*, microfluidic platforms were developed to capture cancer and stromal cells and study their interactions at a single-cell level.[17,18] Similarly, other microfluidic approaches have aided in understanding the role of cancer-associated fibroblasts (CAFs) on cancer cell migration[19] in creating a proangiogenic environment[20] for a cancer-stem cell niche.[21] These systems have significantly improved our understanding about the interactions between cancer and stromal cells such as CAFs both at a single-cell level and studying their heterotypic interactions. Despite these advantages, the scalability of microfluidic devices to study chemotherapeutic drug response requires parallel fluid circuits and likely automation, which is not currently standard practice in pharmaceutical screening facilities. Thus, an *in vitro* model that is high throughput in microwell screening formats, easy to fabricate, and can control the interaction of cancer cells and the cellular components of the tumor microenvironment continues to be of value.

This study expands on previously published work from our group by Shen *et al*, which developed a novel *in vitro* microengineered tumor-stromal assay (μTSA) platform for studying the spatial interaction of breast cancer cell lines and fibroblasts.[22] The μTSA is a coculture system whereby cancer and stromal cells are precisely localized using micropatterning, a technique that has been extensively developed for other cell culture applications to study cell morphogenesis and differentiation.[23,24] Herein, we adapted μTSA to study patient-derived pancreatic cancer and stromal cells. Furthermore, we developed new image-based end points to measure the expansion of micropatterned tumor islands during states of migratory growth or drug treatment. The effect of inhibiting bromodomain and extraterminal (BET) inhibitor was finally evaluated on the population dynamics of tumor and stromal cells in μTSA.

Materials and Methods

Cells and Reagents

Patient-derived 1319-3-NE (pancreatic cancer cell line) was generated from a PDX model of pancreatic ductal adenocarcinoma.[25] The cell line was generated and used in our study after obtaining institutional review board approval (2003P001289) and patient consent. HPDE-6/E6E7 (pancreatic epithelial cells) were generated using the procedure outlined in the study by Ouyang *et al*.[26] JD-PDAC-CAF (pancreatic CAF) were isolated from a human pancreatic adenocarcinoma resected by pancreatoduodenectomy using the Bachem outgrowth method.[27] For all our experiments, we used cells from passages 1 to 6 to maintain consistency. Cell type and purity was assessed by morphology and immunofluorescent staining for vimentin and pan-cytokeratin as described (prognostic significance of zinc-finger E-box binding homeobox 1) expression in cancer cells and CAFs in pancreatic head cancer).[28]

Normal human dermal fibroblasts (NHDFs) were purchased from ATCC. 1319-3-NE were maintained in Dulbecco's modified Eagle medium (DMEM) F12 media with 10% fetal bovine serum (Gibco, USA) and 1% penicillin-streptomycin. HPDE-6/E6E7 cells were cultured in 1× keratinocyte serum-free media (Gibco, USA) supplemented with pituitary bovine serum, epithelial growth factor (EGF), and 1% penicillin-streptomycin. Both NHDF and JD-PDAC CAF cells were cultured in DMEM media supplemented with 10% fetal bovine serum and 1% penicillin-streptomycin. All the reagents for cell culture were purchased from Thermofisher Scientific (USA), unless otherwise specified.

For the imaging experiments, 1319-3NE, HPDE-6/E6E7 cells, NHDF, and JD-PDAC CAF were transduced with lentivirus carrying either mCherry or EGFP reporter genes, respectively. Lentivirus was added to cultures at multiplicities of infection in the range of 2.5 to 5. After 48 hours, the virus-infected cells were purified using flow cytometry at the Massachusetts General Hospital (MGH) flow cytometry core facility.

Micropattern Fabrication

A microtumor stromal assay was fabricated using the previously published method[22] and shown in schematic form in Figure 1. In brief, 12 mm diameter coverslips were cleaned and treated with oxygen plasma (PDC-32G, Harrick Plasma,

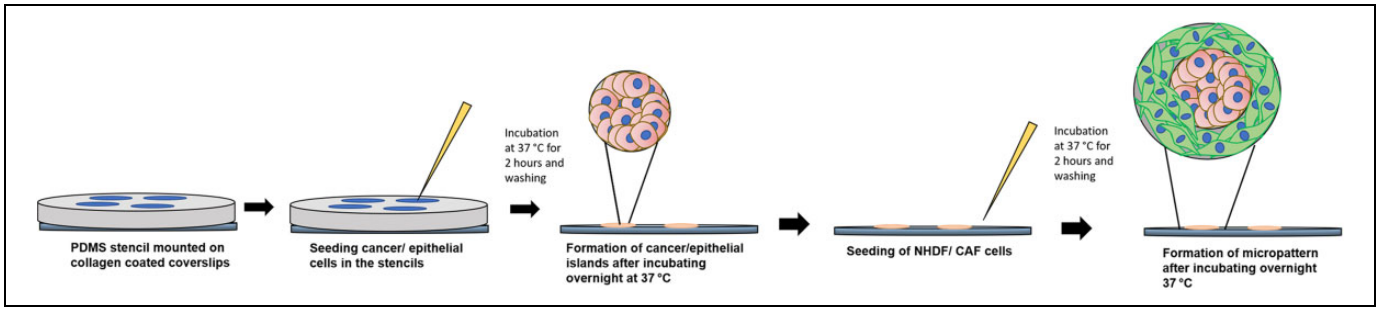

Figure 1. Generation of tumor–stromal micropatterns. Schematic representation of generating the micropatterns using PDMS stencils and epithelial/cancer cells (islands) surrounded by NHDF/CAF (stromal cells). CAF indicates cancer-associated fibroblast; NHDF, normal human dermal fibroblast; PDMS, polydimethylsiloxane.

USA) for 5 minutes. Following this, they were immersed in 1% N-(2-aminoethyl)-3-aminopropyl-trimethoxy-silane (Sigma Aldrich, USA) for 15 minutes. After a series of thorough washing, they were dried with nitrogen gas and then incubated at 100°C for 1 hour. The silanized coverslips were treated with rat tail collagen I extracted in lab, diluted to a concentration of 1 mg/ml in 0.1% acetic acid overnight at 4°C. After the collagen treatment, the coverslips were air dried in a sterile laminar flow hood and sterilized using ultraviolet for half an hour. Polydimethylsiloxane (PDMS) stencils of varying circle diameters (P1-P4) were prepared using the previously published protocol.[22] The stencils of format P2 was used throughout the study unless specified. They were mounted on collagen-coated coverslips and treated for 1 hour in 0.2% (w/v) Pluronic F-127 (Sigma Aldrich, USA) in phosphate-buffered saline (PBS) followed by washing with PBS. Pluronic treatment was done on the micropatterns to prevent protein adhesion in regions other than the PDMS stencil.[29] The tumor–stromal micropatterns were established following the steps illustrated in Figure 1. Cancer and/or epithelial cells were seeded at a density of 0.3×10^6 cells/micropattern and incubated in keratinocyte serum-free media at 37°C for 2 hours. Following this incubation, the patterns were washed with warm media. The stencils were then incubated at 37°C and 5% CO_2 overnight. For the experiments with monoculture cells, the stencils were removed, and time-dependent imaging was performed over a period. In the case of the microtumor stromal assay, the stencils were removed and NHDF GFP/PDAC CAF GFP cells were seeded at a density of 80 000 cells/ micropattern and incubated in keratinocyte serum-free media at 37°C for 1 hour. Following this incubation, the patterns were washed with warm media to remove fibroblast/CAF cells adhering on the cancer/epithelial islands. The patterns were then incubated overnight at 37°C and 5% CO_2. After stabilization of the micropatterns overnight, the media are switched to DMEM F12 containing 10% FBS and 1% pen-strep. The micropatterns were cultured in these media till day 5 with a 10% media change every day.

Determination of Migration of Cells in the Micropattern

The micropatterns of cancer/epithelial cells from the islands were imaged every 24 hours for a period of 3 days using the Axio Zoom V.16 (Zeiss). In the case of monoculture patterns, the migration of cancer and epithelial cells in the absence of stroma was determined. The percent area of cancer islands was determined by selecting the mCherry channel images and analyzing the images using NIH imageJ (version 1.51) following the steps outlined in Figure S1A. Thus, by imaging the same island over time and measuring the percent of cancer cells, the increase in island area (migration) was estimated.

For the micropatterns consisting of cancer cells cocultured with NHDF/CAFs, the migration of cells was characterized in 2 ways using NIH ImageJ software: (1) the number of CAFs/NHDFs within the cancer island and (2) total percent of fibroblasts in the micropattern. For the first method, the number of CAFs/NHDFs within the cancer island were determined by selecting the GFP channel images and analyzing using ImageJ software. Thresholding and island area selection were performed using the steps outlined in Figure S1B. For the second method, the total percent CAFs/NHDF in the micropattern was determined by selecting the GFP channel images. The thresholding and area selection were performed to select the entire area of the image and the percent CAFs/NHDFs was estimated. For both these methods, images of the same islands over time were captured and image analysis was performed. Thus, the analysis over time provided the percent CAFs/NHDF or number of fibroblast over time.

Pharmacological Treatment of Cancer Cell Cocultures

The BET inhibitor, CPI 203 (Constellation Pharmaceuticals, USA) at a concentration of 1.4 μM was added to the micropatterns with cancer cells cocultured with CAFs. The control micropatterns were treated with dimethyl sulfoxide (DMSO). The migration of cancer cells in the control and drug-treated group was determined by tracking the micropatterns over time and analyzing the island size NIH ImageJ as described above.

Statistics

The results are reported as mean (standard deviation; n = 4-6 islands from 2 to 3 independent experiments). Statistical significance between multiple groups was calculated using 1-way or 2-way analysis of variance for multiple comparisons followed by

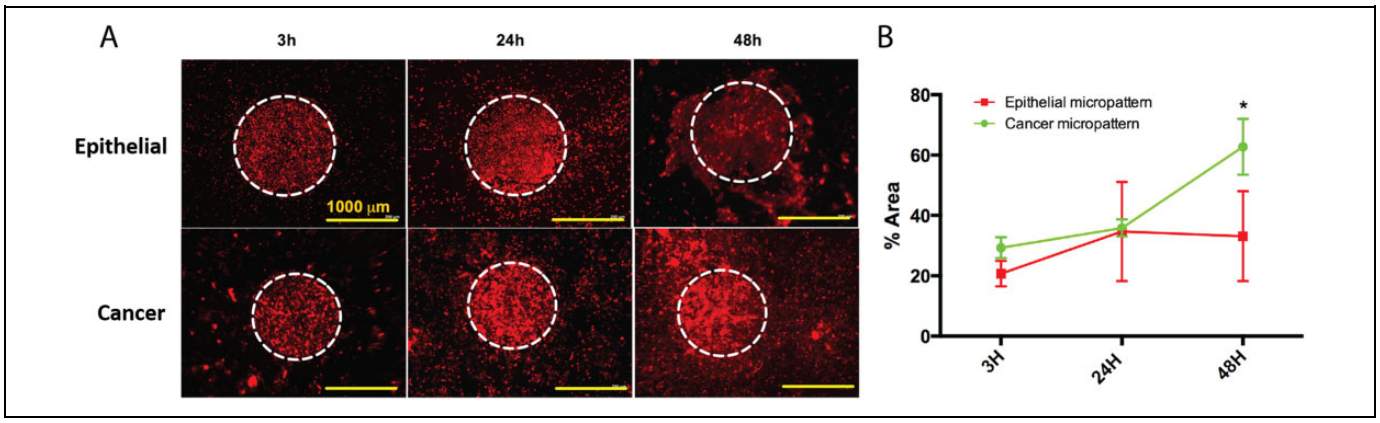

Figure 2. Migration of normal patient-derived epithelial cells versus cancer cells. Pancreatic epithelial cells (HPDE6/E6E7) expressing mCherry and pancreatic cancer cells (1319-3-NE) were seeded on PDMS stencils to form respective epithelial/cancer islands. A, Fluorescent images of the micropatterns taken at different time points ranging from 3 to 48 hours. B, ImageJ analysis of percent area occupied by cancer/epithelial cells at each time point in terms of data (SD; n = 5-6 cancer/epithelial islands). * denotes statistical significance when compared to the control epithelial island ($P < .05$). PDMS indicates polydimethylsiloxane; SD, standard deviation.

Tukey post hoc analysis (Graphpad prism, version 6). P values less than .05 were considered statistically significant.

Results

Increased Migration of Patient Pancreatic Cancer Cells Compared to Normal Patient-Derived Epithelial Cells

The µTSA was first tested to develop analytical methods to study circumferential cell migration as a new quantitative end point of the assay. The inherent migratory potential of the patient-derived cancer cell line 1319-3-NE was first studied in µTSA using islands of cancer cells in the absence of any stromal cells. A noncancerous cell line was also derived from pancreatic epithelial cells (HPDE6/E7) as a normal epithelial cell control. To facilitate tracking of cell migration, HPDE6 and 1319-3-NE cells were infected with lentivirus that express mCherry-fluorescent protein. Cancer or epithelial islands were formed using the PDMS stencils mounted on collagen-coated coverslips. After 24 hours, the PDMS stencils were removed and the migration of cancer and epithelial cells from their respective micropattern was imaged at 3, 24, and 48 hours as shown in Figure 2A. The extent of migration was quantified using ImageJ analysis as shown in Figure 2B. The migration of cancer cells was significantly greater than normal epithelial cells by 48 hours ($P \leq .05$). This result qualified this end point assay for the study of migration between cancerous cells and their normal counterparts.

Increased Interfacial Interactions Between Tumor and Stroma Can Cause an Invasive Switch

Pancreatic cancer has a large number of fibroblastic cells contributing to the tumor microenvironment. Hence, we investigated the behavior of tumor cells in the presence of fibroblasts. For these experiments, we used NHDF cells that were engineered to express GFP using lentivirus. The goal of this study was to evaluate the migration of cancer cells with increasing amounts of heterotypic interaction with neighboring fibroblasts. Stencils of different circle diameters (P1-P4) were used for this experiment, which assured that the same total number of tumor and fibroblastic cells were maintained on each pattern (Figure 3A). The total area of all the circles in each stencil type remained constant; however, the individual area of each circle was different in the patterns P1 to P4, with P1 having the largest area and P4 being the smallest in terms of cancer cells per island. Owing to the differences in the number of circles in the stencils, P4 had the highest surface area of interaction between cancer and stromal cells as shown in Figure 3B. The migration of cancer cells in the presence of NHDF cells in the stencils P1 to P4 was tracked over a period of 4 days with the highest migration of cancer islands taking place in P4 patterns with the most amount of heterotypic stromal interaction (Figure 3C). A disorganized and invasive morphology was observed in P4 whereas most other patterns maintained a relatively circular migration pattern. These studies confirm a stark increase in cell migration that is primarily instigated by more interfacial interaction with NHDFs rather than a total number of stromal cells.

Type of Stroma Dictates the Tumor Progression

Cancer tissue is heterogeneous with different types of stromal cells localized in the tumor microenvironment.[30] To study the role of specific fibroblastic subtypes, we studied the response of 1319-3-NE cells cocultured with normal fibroblasts versus CAFs and measured the migration of tumor cells. These experiments employed a µTSA pattern (P2) in which NHDFs had minimal effects on cancer cell migration. As shown in Figure 4A, the migration of cancer cells in the presence of JD-PDAC CAFs is higher when compared to the NHDF coculture by 48 hours and quantified by image analysis of the area of the cancer island per high image field (Figure 4B).

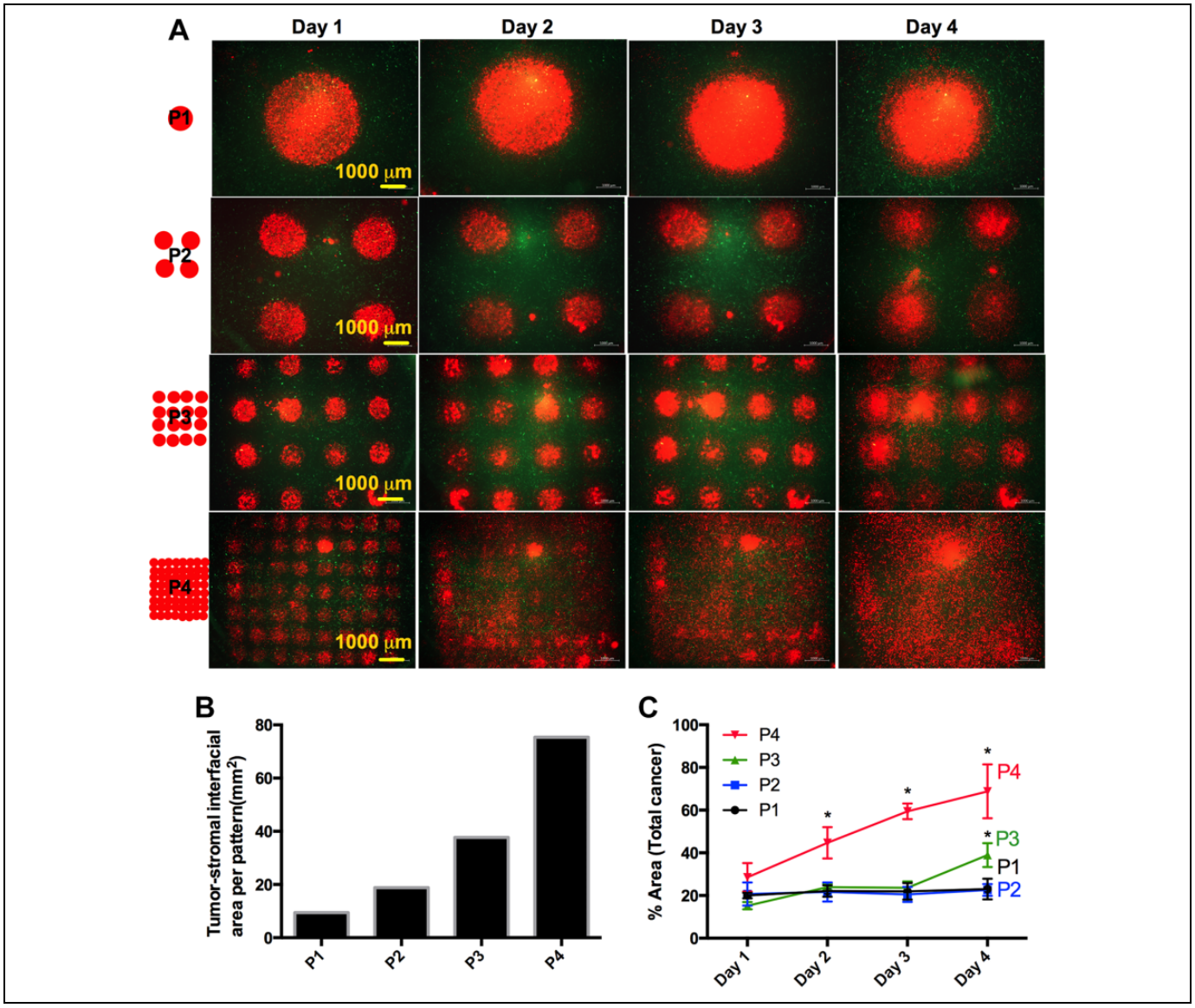

Figure 3. Pancreatic cancer cells (1319-MP3-NE mCherry) were seeded in PDMS stencils of varying circle diameters (P1-P4) and cocultured with normal dermal fibroblast (NHDF-GFP). P1, P2, P3, and P4 were 3, 1.5, 0.75, and 0.375 mm, respectively; center-to-center distances were 4, 2, and 1 mm for P2, P3, and P4, respectively. A, Representative fluorescent images of the micropatterns taken at different time points from day 1 to day 4. B, Quantification of the total tumor–stromal interfacial area in each stencil type. C, Migration of cells from the cancer islands using stencils with different tumor–stromal interfacial areas calculated using ImageJ analysis of the images taken at different time points. The increased interfacial area in P4 correlates with the increase in migration of cells. The figure represents data (SD; n = 3-4 micropatterns/condition). * denotes statistical significance when compared to the P1 micropattern ($P < .05$). PDMS indicates polydimethylsiloxane; SD, standard deviation.

In addition to the migration of the cancer cells, we observed an expansion of fibroblasts into cancer islands. This expansion of fibroblasts was calculated based on the number of NHDFs/CAFs located inside the cancer island over time. In contrast to their differential effects on the migration of 1319-3-NE cells, both normal dermal fibroblasts and CAFs increased in number in the cancer island with comparable efficiency (Figure 4C). This system can not only be used in studying the role of different stromal cells on functional end-point like migration but also provide an insight on the 2-way cellular interactions of fibroblasts that likely occurs within a tumor microenvironment.

Bromodomain and Extraterminal Inhibition Impacts Both Tumor and Stroma in a Spatiotemporal Manner

Members of the BET domain family of chromatin adaptors (BRD2, BRD3, and BRD4) play key roles promoting the growth of both the neoplastic and stromal cells in PDAC tumors.[13] For validating the µTSA model as a drug screening

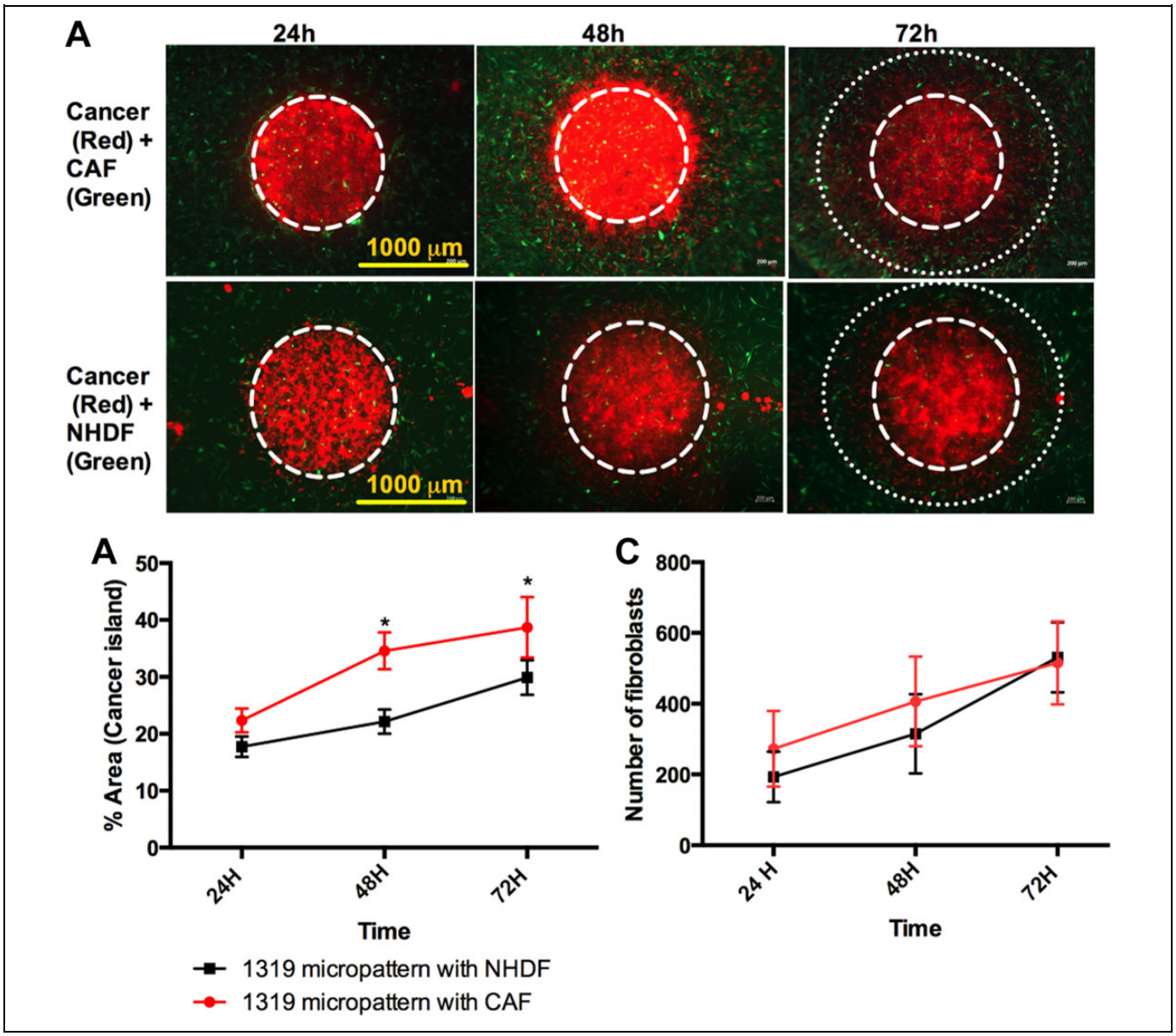

Figure 4. Stromal type instigates cancer migration. Pancreatic cancer cells (1319-MP3-NE mCherry) were seeded in PDMS stencils and cocultured with normal dermal fibroblast (NHDF-GFP) or patient-derived pancreatic cancer associated fibroblast (CAF-GFP). A, Fluorescent images of the micropatterns taken at different time points ranging from 24 to 72 hours. The presence of CAFs increase the migration of cancer cells. B, C, ImageJ analysis on the images in terms of data (SD; n = 5-6 cancer islands). * denotes statistical significance when compared to the NHDF group ($P < .05$). PDMS indicates polydimethylsiloxane; SD, standard deviation.

platform, we cultured the 1319-3-NE cancer cells with CAFs and evaluated the pan-BET inhibitor, CPI203, that prevents the binding of the BET proteins to their targets acetylated lysines on histones. CPI203 has been shown to dramatically reduce pancreatic cancer growth *in vitro* and *in vivo* by Huang *et al*,[31] though it is unknown what CPI203 does to stromal cells. After stabilizing the micropattern culture for 24 hours with serum-containing media, the patterns were divided into 2 groups, one treated with BET inhibitor 1.4 µM and the other with DMSO control. The concentration of this drug was chosen based on the dose–response curve for the viability of cancer cells treated with CPI203 treated for 5 days (Figure S2). Patterns treated with BET inhibitor showed a decrease in the size of cancer island area over a period of 72 hours (Figure 5A). In DMSO-treated groups, cancer islands continued to grow and CAFs were evident. The area of cancer islands in the BET inhibitor treated group was 20.63% (3.41%) when compared to a 68.13% (7.92%) in the DMSO-treated group at 48 hours (Figure 5B). Interestingly, the total number of CAFs were also eliminated by the treatment within a similar timescale (Figure 5C). These results demonstrate the applicability of µTSA model to spatially study multiple cell populations during drug exposure.

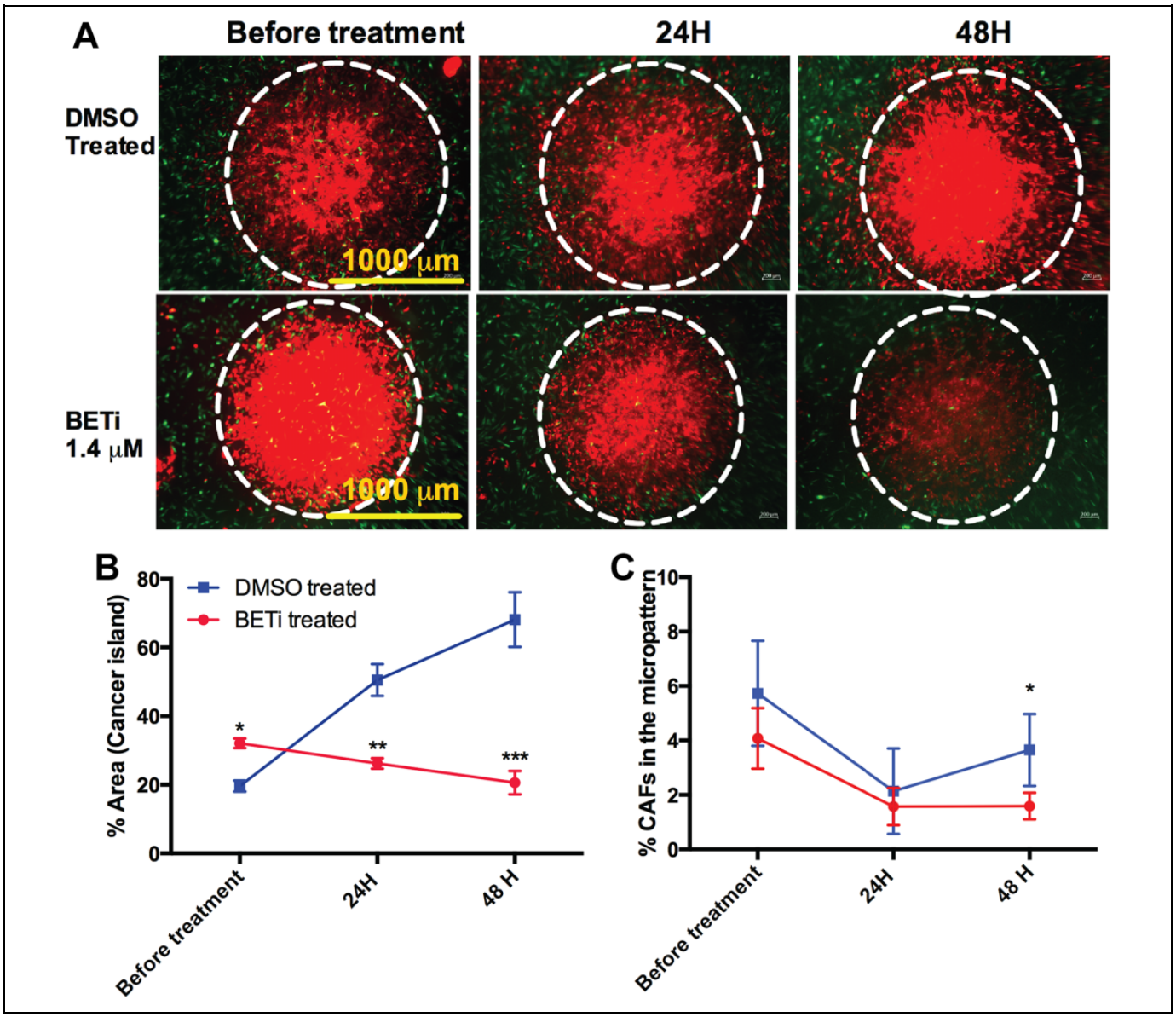

Figure 5. Pharmacological inhibition of growth using BET inhibitor. μTSA of patient-derived pancreatic cancer and CAF cells treated with 1.4 μM BET inhibitor or DMSO controls. A, Representative images of the micropatterns taken before and after BET inhibitor/DMSO at different time points. B, ImageJ analysis of the percent area occupied by the cancer cells over time following DMSO/drug treatment. Treatment with BET inhibitor decreased the viability of cancer cells by approximately 60% marked by the shrinking of cancer islands. C, ImageJ analysis of percent area occupied by the cancer associated fibroblast in the whole micropattern. The ImageJ quantification represented here are based on average (SD; n = 5-6 cancer islands/condition) and *, **, and *** represent statistical significance when compared to the control DMSO-treated group at the respective time points. BET indicates bromodomain and extraterminal; CAF, cancer-associated fibroblast; DMSO, dimethyl sulfoxide; SD, standard deviation; μTSA, microengineered tumor stromal assay.

Discussion

New models that account and control for the stromal component of a tumor microenvironment can provide new insight into cancer biology. Characteristic of pancreatic adenocarcinoma is a highly desmoplastic stroma, composed of abundant fibrosis, CAFs, leaky abnormal blood vessels, and infiltrating immune cells.[32] This pronounced stromal desmoplasia not only promotes the aggressive local growth of the tumor and the intrinsic chemoresistance of cancer cells[33,34] but also acts as a physical barrier to effective chemotherapeutic targeting.[35,36] Much of the focus of the tumor microenvironment of PDAC has been on the cellular components, revealing that CAFs promote tumor formation during early tumor development, but serve to restrain cancer cell growth in established tumors.[37-40] This study evaluated a desmoplastic coculture of patient-derived tumor cells with a focus on imaging population dynamics in a spatially controlled micropatterned culture.

We first validated enhanced migratory potential of patient-derived cancer cells compared to their epithelial cell controls. The use of μTSA for cell migration studies is beneficial because of the opportunity to visualize tumor cells in real-time during an "invasion" process into a stromal compartment. In comparison, commonly used systems such as Boyden chamber assay to determine migration of cancer cells in the presence of chemoattractants do not account for cell–cell contact and real-time tracking of cell migration cannot be accomplished using this method.[41] Furthermore, we also could study the fate of fibroblasts into a tumor bed. Although it is unclear whether fibroblasts migrated into the cancer island from the periphery or a small initial population initially embedded in the cancer island grow within the pattern, stromal penetration into tumors is a critical process that is actively driven by tumor cells to shape their microenvironment into a growth supportive and immunosuppressive environment which can be specifically explored in future studies.

Using μTSA, we could study, for the first time, the amount of heterotypic interfacial interactions and its influence on cancer cell migration. By varying island density with a fixed number of total cancer and stromal cells, our studies indicate that the increase in tumor–stromal interfacial area led to increased aggressiveness of the tumor at a specific tipping point. From our previously published study with MDA-MB231 breast cancer cells cocultured with NHDF in patterns with varying stencil patterns, we observed a contact mediated increase in chemokine (C-C motif) ligand 5 (CCL5) and interleukin-6 (IL6) activation of stromal cells by cancer cells. The increase in interfacial surface area correlated with an increase in CCL5 and IL6.[22] Growth factors such as tumor growth factor-β1, C-X-C motif chemokine 12,[42] platelet-derived growth factor-α/β,[43] and IL6 secreted by cancer cells are involved in the activation of fibroblast in the tumor stroma. The loss of critical tumor suppressor genes such as *PTEN*, *CAV-1*,[43] *p53*, and *p21* in resident fibroblast of the tumor are also involved in the activation process.[43] Franci *et al* demonstrated that SNAIL, an important protein that is involved in epithelial–mesenchymal transition and invasion of tumor cells, is upregulated at the tumor–stromal interface.[44] Collectively, these results suggest that the co-opting of a normal fibroblast phenotype into a CAF phenotype may occur at a critical point at which interfacial interactions go beyond a threshold. Genomic profiling of fibroblasts in different patterns for changes in activation genes is warranted in future studies.

The type of fibroblastic stroma was prospectively studied in μTSA with patient-derived cancer cells where it was observed that CAFs instigate tumor migration more so than NHDFs. A study by Gao *et al* demonstrated that MDA-MB321 cells cultured with conditioned media from fibroblasts isolated CAFs from a tumor–stromal interface showed increased tumor migration when compared to the cocultures with normal fibroblast media.[45] Similarly, a study by Shan *et al* probed into the invasiveness of pancreatic cancer cell lines PANC-1 and BxPc-3 in the presence of CAF/normal fibroblast conditioned media using transwell and scratch assay, respectively. In both these assays, CAFs promoted the migration and invasion of cancer cells.[46] Thus, these studies showed similar trends of CAF instigating cancer cell migration using invasion assays.

The BET family of chromatin adaptors plays a key role in regulating the expression of the matrix molecules in both stromal and cancer cells of patient-derived xenograft tumors.[31] *In vivo* antitumor effects of BET inhibitors were rather dependent on the suppression of tumor-promoting activity in CAFs.[47] Our study visualized the co-evolution of BET inhibition on both tumor and stromal cells and found a striking and concordant loss of both cells types in response to BET blockade. Uncoupling of the spatial and temporal dynamics of this response in each cell type can be an important follow-up to understand the multistep process by which BET inhibitors act.

In conclusion, we adapted and evolved μTSA for use with patient-derived cells. This controlled coculture method revealed important triggers of tumor cell viability and growth that included the type of stroma, amount of heterotypic interaction, and coordinated response to a small molecule inhibitor that was enabled by having precise control of tumor–stromal interactions.

Authors' Note

The cancer cells used this study were obtained from patients after approval from the institutional review board and patient consent and all the methods were performed as per institutional guidelines. This study applied a novel microengineered tumor assay to model and visualize the interactions between patient-derived cancer cells and their fibroblastic neighbors.

Declaration of Conflicting Interests

The author(s) declared no potential conflicts of interest with respect to the research, authorship, and/or publication of this article.

Funding

The author(s) disclosed receipt of the following financial support for the research, authorship, and/or publication of this article: This work was supported in part by the Shriners Hospitals for Children (BP), and National Institutes of Health grant R01EB012521 (BP).

ORCID iD

Biju Parekkadan, PhD http://orcid.org/0000-0002-3408-8085

Supplemental Material

Supplemental material for this article is available online.

References

1. Kaur S, Baine MJ, Jain M, Sasson AR, Batra SK. Early diagnosis of pancreatic cancer: challenges and new developments. *Biomark Med*. 2012;6(5):597-612.
2. Bissell MJ, Hines WC. Why don't we get more cancer? A proposed role of the microenvironment in restraining cancer progression. *Nat Med*. 2011;17(3):320-329.
3. Hanahan D, Weinberg Robert A. Hallmarks of cancer: the next generation. *Cell*. 2011;144(5):646-674.
4. Öhlund D, Elyada E, Tuveson D. Fibroblast heterogeneity in the cancer wound. *J Exp Med*. 2014;211(8):1503-1523.

5. Bussard KM, Mutkus L, Stumpf K, Gomez-Manzano C, Marini FC. Tumor-associated stromal cells as key contributors to the tumor microenvironment. *Breast Cancer Res*. 2016;18(1):84.
6. Yee NS, Ignatenko N, Finnberg N, Lee N, Stairs D. Animal models of cancer biology. *Cancer Growth Metastasis*. 2015;8(suppl 1):115-118.
7. Hirschhaeuser F, Menne H, Dittfeld C, West J, Mueller-Klieser W, Kunz-Schughart LA. Multicellular tumor spheroids: an underestimated tool is catching up again. *J Biotechnol*. 2010;148(1): 3-15.
8. Hu M, Yao J, Cai L, et al. Distinct epigenetic changes in the stromal cells of breast cancers. *Nat Genet*. 2005;37(8):899-905.
9. Kidd S, Spaeth E, Watson K, et al. Origins of the tumor microenvironment: quantitative assessment of adipose-derived and bone marrow-derived stroma. *PLoS One*. 2012;7(2):e30563.
10. Mak IW, Evaniew N, Ghert M. Lost in translation: animal models and clinical trials in cancer treatment. *Am J Transl Res*. 2014;6(2): 114-118.
11. Schuh JC. Trials, tribulations, and trends in tumor modeling in mice. *Toxicol Pathol*. 2004;32(1 suppl):53-66.
12. Mosaad EO, Chambers KF, Futrega K, Clements JA, Doran MR. The microwell-mesh: a high-throughput 3D prostate cancer spheroid and drug-testing platform. *Sci Rep*. 2018;8(1):253.
13. Tung YC, Hsiao AY, Allen SG, Torisawa YS, Ho M, Takayama S. High-throughput 3D spheroid culture and drug testing using a 384 hanging drop array. *Analyst*. 2011;136(3):473-478.
14. Chen YC, Lou X, Zhang Z, Ingram P, Yoon E. High-throughput cancer cell sphere formation for characterizing the efficacy of photo dynamic therapy in 3D cell cultures. *Sci Rep*. 2015;5: 12175.
15. Yamada KM, Cukierman E. Modeling tissue morphogenesis and cancer in 3D. *Cell*. 2007;130(4):601-610.
16. Thoma CR, Zimmermann M, Agarkova I, Kelm JM, Krek W. 3D cell culture systems modeling tumor growth determinants in cancer target discovery. *Adv Drug Deliv Rev*. 2014;69:29-41.
17. Hong S, Pan Q, Lee LP. Single-cell level co-culture platform for intercellular communication. *Integr Biol (Camb)*. 2012;4(4): 374-380.
18. Chen Y-C, Zhang Z, Fouladdel S, et al. Single cell dual adherent-suspension co-culture micro-environment for studying tumor–stromal interactions with functionally selected cancer stem-like cells. *Lab Chip*. 2016;16(15):2935-2945.
19. Mi S, Du Z, Xu Y, et al. Microfluidic co-culture system for cancer migratory analysis and anti-metastatic drugs screening. *Sci Rep*. 2016;6:35544.
20. Lee SW, Kwak HS, Kang M-H, Park YY, Jeong GS. Fibroblast-associated tumour microenvironment induces vascular structure-networked tumouroid. *Sci Rep*. 2018;8(1):2365.
21. Yu T, Guo Z, Fan H, et al. Cancer-associated fibroblasts promote non-small cell lung cancer cell invasion by upregulation of glucose-regulated protein 78 (GRP78) expression in an integrated bionic microfluidic device. *Oncotarget*. 2016;7(18): 25593-25603.
22. Shen K, Luk S, Hicks DF, et al. Resolving cancer–stroma interfacial signalling and interventions with micropatterned tumour–stromal assays. *Nat Commun*. 2014;5:5662.
23. Bhatia SN, Balis UJ, Yarmush ML, Toner M. Microfabrication of hepatocyte/fibroblast co-cultures: role of homotypic cell interactions. *Biotechnol Prog*. 1998;14(3):378-387.
24. El-Ali J, Sorger PK, Jensen KF. Cells on chips. *Nature*. 2006; 442(7101):403-411.
25. Pergolini I, Morales-Oyarvide V, Mino-Kenudson M, et al. Tumor engraftment in patient-derived xenografts of pancreatic ductal adenocarcinoma is associated with adverse clinicopathological features and poor survival. *PLoS One*. 2017;12(8): e0182855.
26. Ouyang H, Mou LJ, Luk C, et al. Immortal human pancreatic duct epithelial cell lines with near normal genotype and phenotype. *Am J Pathol*. 2000;157(5):1623-1631.
27. Bachem MG, Schneider E, Groß H, et al. Identification, culture, and characterization of pancreatic stellate cells in rats and humans. *Gastroenterology*. 1998;115(2):421-432.
28. Bronsert P, Kohler I, Timme S, et al. Prognostic significance of zinc finger E-box binding homeobox 1 (ZEB1) expression in cancer cells and cancer-associated fibroblasts in pancreatic head cancer. *Surgery*. 2014;156(1):97-108.
29. Rodriguez NM, Desai RA, Trappmann B, Baker BM, Chen CS. Micropatterned multicolor dynamically adhesive substrates to control cell adhesion and multicellular organization. *Langmuir*. 2014;30(5):1327-1335.
30. Ronnov-Jessen L, Petersen OW, Bissell MJ. Cellular changes involved in conversion of normal to malignant breast: importance of the stromal reaction. *Physiol Rev*. 1996;76(1):69-125.
31. Huang Y, Nahar S, Nakagawa A, et al. Regulation of GLI underlies a role for BET bromodomains in pancreatic cancer growth and the tumor microenvironment. *Clin Cancer Res*. 2016;22(16): 4259-4270.
32. Erkan M, Hausmann S, Michalski CW, et al. The role of stroma in pancreatic cancer: diagnostic and therapeutic implications. *Nat Rev Gastroenterol Hepatol*. 2012;9(8):454-467.
33. Miyamoto H, Murakami T, Tsuchida K, Sugino H, Miyake H, Tashiro S. Tumor–stroma interaction of human pancreatic cancer: acquired resistance to anticancer drugs and proliferation regulation is dependent on extracellular matrix proteins. *Pancreas*. 2004;28(1):38-44.
34. Muerkoster S, Wegehenkel K, Arlt A, et al. Tumor stroma interactions induce chemoresistance in pancreatic ductal carcinoma cells involving increased secretion and paracrine effects of nitric oxide and interleukin-1beta. *Cancer Res*. 2004;64(4): 1331-1337.
35. Olive KP, Jacobetz MA, Davidson CJ, et al. Inhibition of Hedgehog signaling enhances delivery of chemotherapy in a mouse model of pancreatic cancer. *Science*. 2009;324(5933): 1457-1461.
36. Provenzano PP, Cuevas C, Chang AE, Goel VK, Von Hoff DD, Hingorani SR. Enzymatic targeting of the stroma ablates physical barriers to treatment of pancreatic ductal adenocarcinoma. *Cancer Cell*. 2012;21(3):418-429.
37. Rhim AD, Oberstein PE, Thomas DH, et al. Stromal elements act to restrain, rather than support, pancreatic ductal adenocarcinoma. *Cancer Cell*. 2014;25(6):735-747.

38. Lee JJ, Perera RM, Wang H, et al. Stromal response to Hedgehog signaling restrains pancreatic cancer progression. *Proc Natl Acad Sci U S A*. 2014;111(30):E3091-E3100.
39. Clark CE, Hingorani SR, Mick R, Combs C, Tuveson DA, Vonderheide RH. Dynamics of the immune reaction to pancreatic cancer from inception to invasion. *Cancer Res*. 2007;67(19): 9518-9527.
40. Collins MA, Bednar F, Zhang Y, et al. Oncogenic Kras is required for both the initiation and maintenance of pancreatic cancer in mice. *J Clin Invest*. 2012;122(2):639-653.
41. Hulkower KI, Herber RL. Cell migration and invasion assays as tools for drug discovery. *Pharmaceutics*. 2011;3(1):107-124.
42. Kojima Y, Acar A, Eaton EN, et al. Autocrine TGF-β and stromal cell-derived factor-1 (SDF-1) signaling drives the evolution of tumor-promoting mammary stromal myofibroblasts. *Proc Natl Acad Sci U S A*. 2010;107(46):20009-20014.
43. Mao Y, Keller ET, Garfield DH, Shen K, Wang J. Stromal cells in tumor microenvironment and breast cancer. *Cancer Metastasis Rev*. 2013;32(1):303-315.
44. Franci C, Takkunen M, Dave N, et al. Expression of Snail protein in tumor–stroma interface. *Oncogene*. 2006;25(37):5134.
45. Gao M-Q, Kim BG, Kang S, et al. Stromal fibroblasts from the interface zone of human breast carcinomas induce an epithelial–mesenchymal transition-like state in breast cancer cells in vitro. *J Cell Sci*. 2010;123(20):3507-3514.
46. Shan T, Chen S, Chen X, et al. Cancer-associated fibroblasts enhance pancreatic cancer cell invasion by remodeling the metabolic conversion mechanism. *Oncol Rep*. 2017;37(4):1971-1979.
47. Yamamoto K, Tateishi K, Kudo Y, et al. Stromal remodeling by the BET bromodomain inhibitor JQ1 suppresses the progression of human pancreatic cancer. *Oncotarget*. 2016;7(38): 61469-61484.